

# *Optical properties of Wigner crystal and helical state in bilayer graphene*

René Côté, Manuel Barrette and Élie Bouffard

Département de physique  
Université de Sherbrooke



UNIVERSITÉ DE  
**SHERBROOKE**



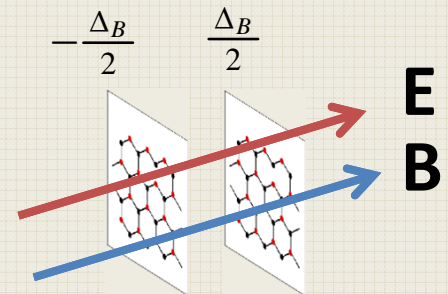
Natural Sciences and Engineering  
Research Council of Canada

Conseil de recherches en sciences  
naturelles et en génie du Canada



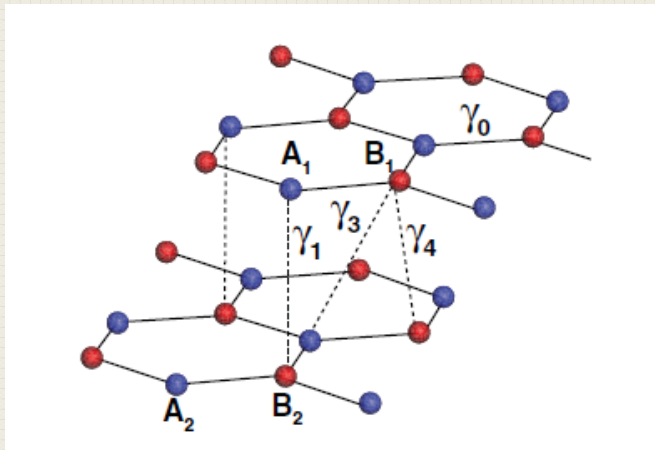
# Outline

Non-collinear orbital pseudomagnetic states can exist in Landau level N=0 of a **biased** graphene bilayer in a magnetic field. They can be detected by optical experiments.



- Origin of the orbital pseudospin in biased bilayer graphene.
- Phase diagram for non-collinear pseudomagnetic states.
- Optical properties: absorption and Kerr effect.

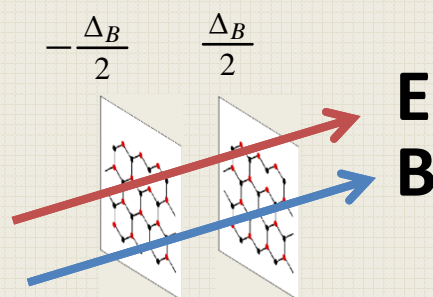
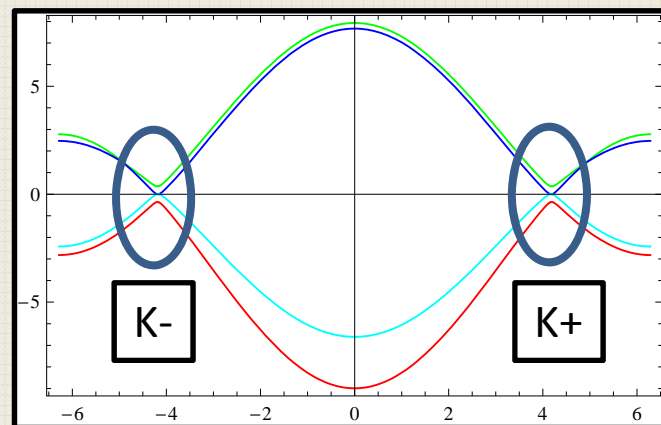
# Bernal-stacked graphene bilayer



A1-B2: high-energy sites  
A2-B1: low-energy sites

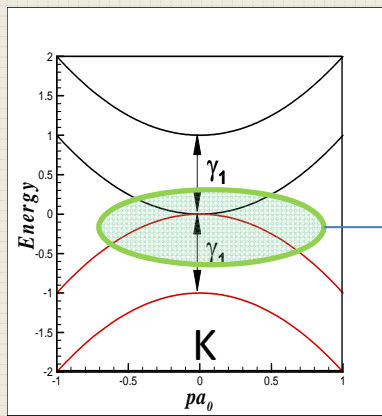
$\gamma_0 = 3.12 \text{ eV}$  n.n intralayer hopping

$\gamma_1 = 0.38 \text{ eV}$  n.n interlayer hopping

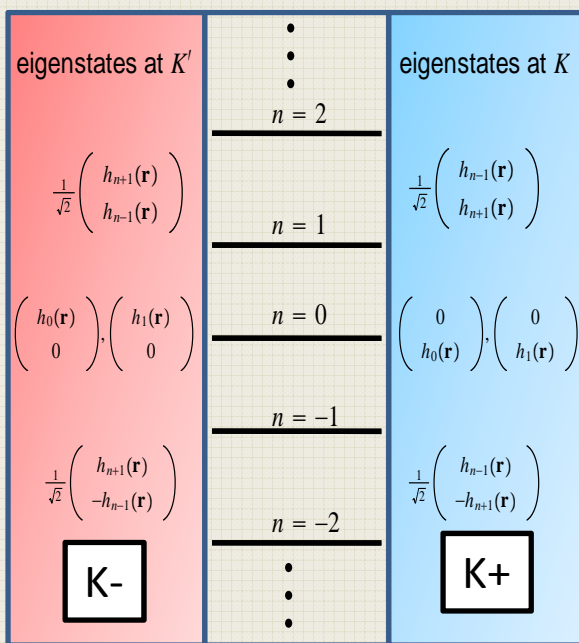


Band structure and the two valleys

# BLG in a magnetic field: Landau levels



→



$$E_n = \pm \hbar\omega_c^* \sqrt{|n|(|n| + 1)}$$

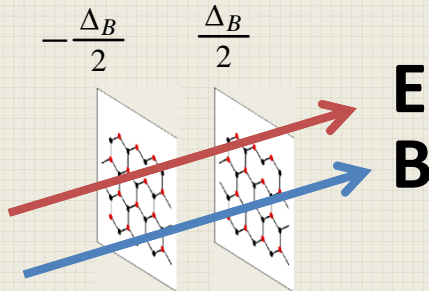
$$n = \dots, -3, 2, -1, 0, 1, 2, 3, \dots$$

$$\begin{pmatrix} A_2 \\ B_1 \end{pmatrix}$$

**Bottom layer**  
**Top layer**

**Two-component model**  
**amplitudes on low-energy sites**

# N=0 Landau level degeneracy



$$h_n(\mathbf{r}) = \frac{1}{\sqrt{L_y}} e^{-iXy/\ell^2} \varphi_n(x - X)$$

orbital

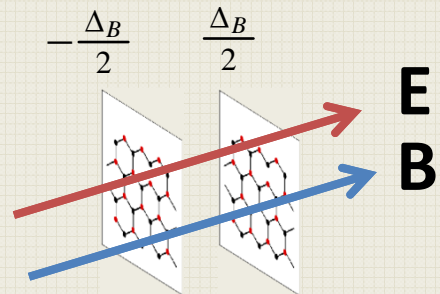
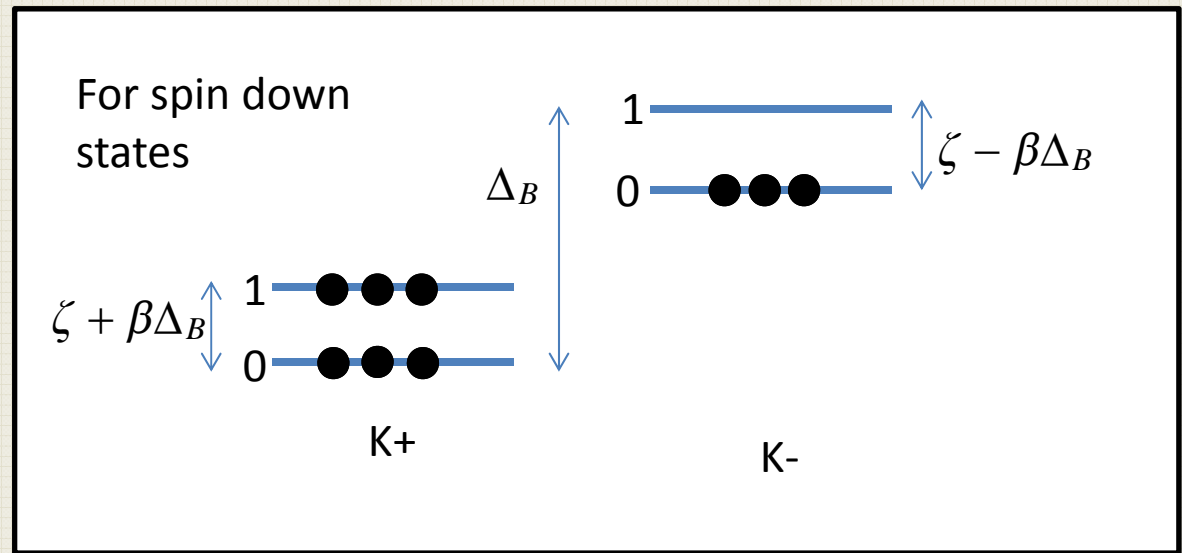
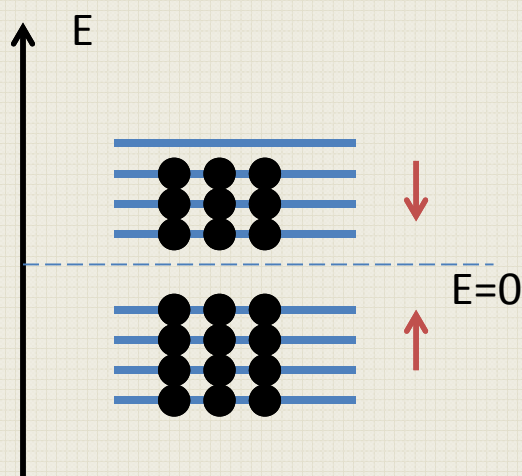
Valley and layer indices  
are related in N=0

	eigenstates at $K'$ $\frac{1}{\sqrt{2}} \begin{pmatrix} h_{n+1}(\mathbf{r}) \\ h_{n-1}(\mathbf{r}) \end{pmatrix}$	$\vdots$ $n = 2$ <hr/> $n = 1$ <hr/>	eigenstates at $K$ $\frac{1}{\sqrt{2}} \begin{pmatrix} h_{n-1}(\mathbf{r}) \\ h_{n+1}(\mathbf{r}) \end{pmatrix}$	
	$\begin{pmatrix} h_0(\mathbf{r}) \\ 0 \end{pmatrix}, \begin{pmatrix} h_1(\mathbf{r}) \\ 0 \end{pmatrix}$	$n = 0$ <hr/>	$\begin{pmatrix} 0 \\ h_0(\mathbf{r}) \end{pmatrix}, \begin{pmatrix} 0 \\ h_1(\mathbf{r}) \end{pmatrix}$	
	$\frac{1}{\sqrt{2}} \begin{pmatrix} h_{n+1}(\mathbf{r}) \\ -h_{n-1}(\mathbf{r}) \end{pmatrix}$	$n = -1$ <hr/> $n = -2$ <hr/> $\vdots$	$\frac{1}{\sqrt{2}} \begin{pmatrix} h_{n-1}(\mathbf{r}) \\ -h_{n+1}(\mathbf{r}) \end{pmatrix}$	

$\begin{pmatrix} A_2 \\ B_1 \end{pmatrix}$  **Bottom layer**  
**Top layer**

Landau level N=0 has 8 sub-levels: 2(spin) X 2(valleys) X 2(orbitals)

# Special case: N=0 and v=3



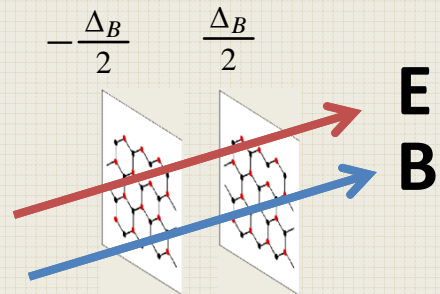
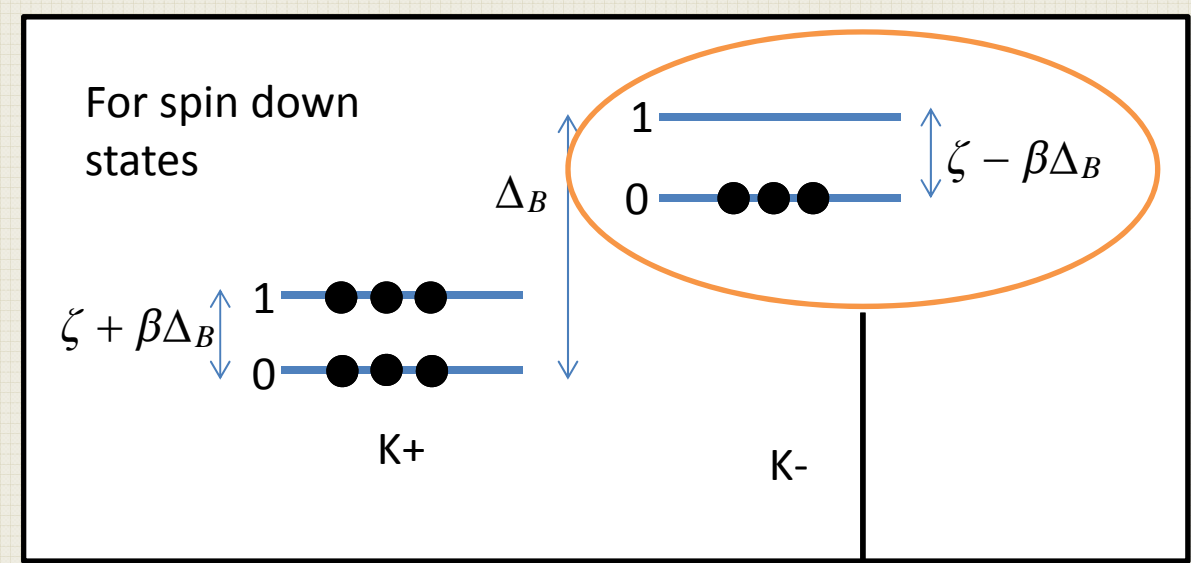
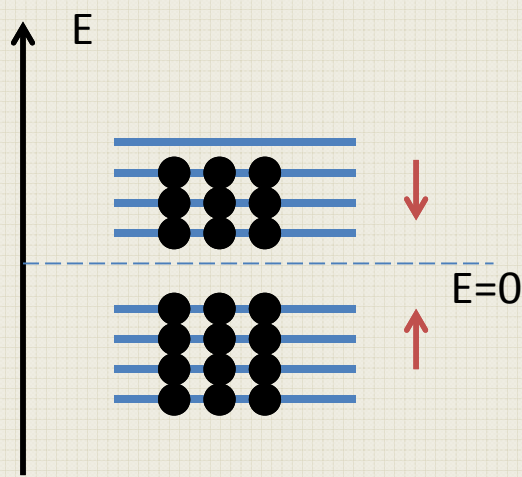
$$\zeta = \beta \left( 2 \frac{\gamma_1 \gamma_4}{\gamma_0} + \delta_0 \right),$$

$$\beta = \frac{\hbar \omega_c^*}{\gamma_1} = 7.24 \times 10^{-3} B[T],$$

$$\zeta = 0.39 B[T] \text{ meV},$$

$$\Delta_Z = 0.12 B[T] \text{ meV}.$$

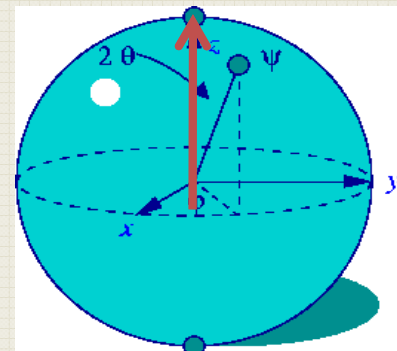
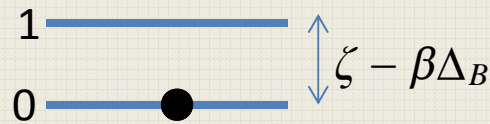
# A two-level system



The 0-1 gap can be made negative !

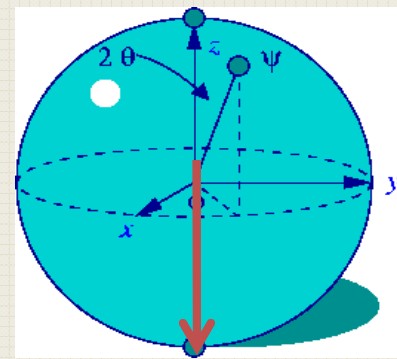
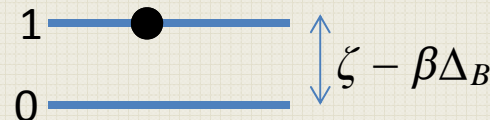
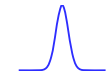
Our two-level system:  
the gap is controlled by the  
electric field between the layers.

# Orbital pseudospin



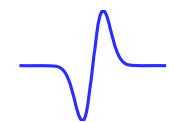
*orbital  $n=0$*

$$\begin{pmatrix} 0 \\ \varphi_0 \end{pmatrix}$$



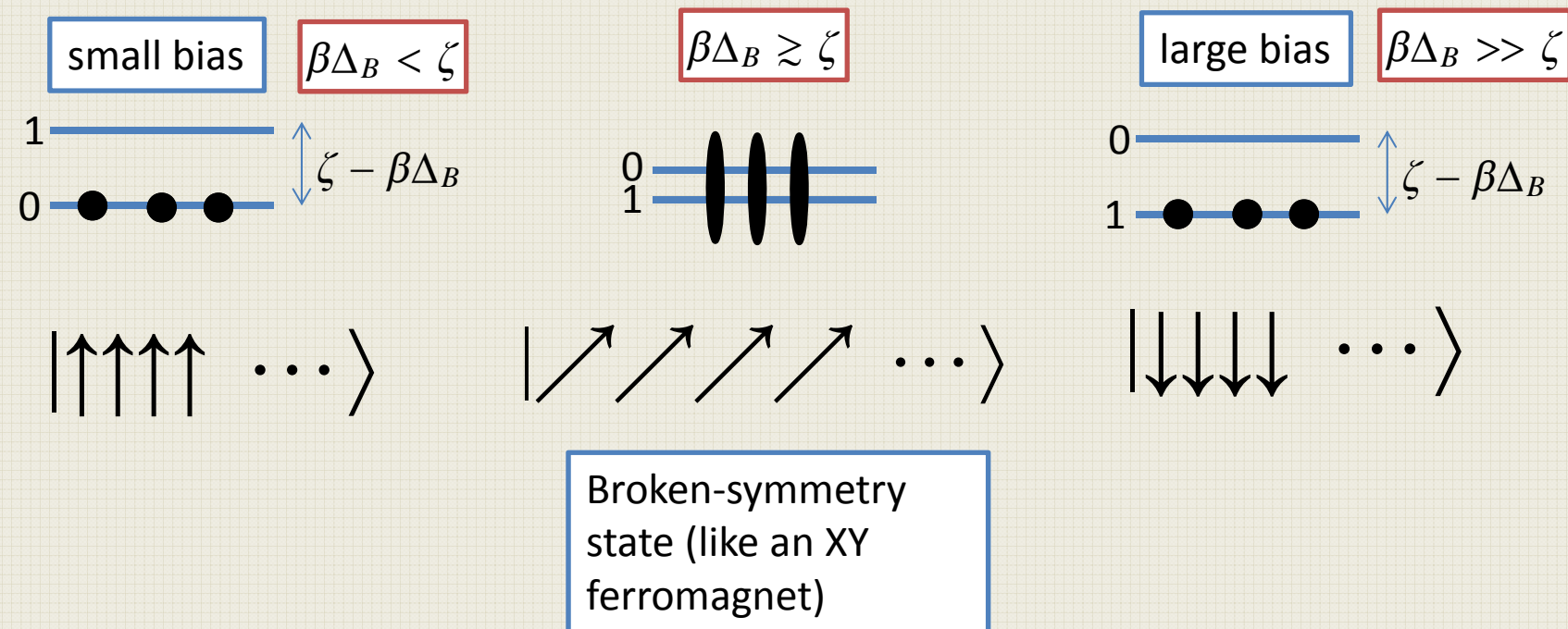
*orbital  $n=1$*

$$\begin{pmatrix} 0 \\ \varphi_1 \end{pmatrix}$$



Quantum mechanics allows any linear combinations of these two states so that the orbital pseudospin can point anywhere on the Bloch sphere.

# Quantum Hall ferromagnetism with orbital pseudospin



Coulomb exchange interaction is more negative for electrons in  $n=0$  than for electrons in  $n=1$

# General Hartree-Fock Hamiltonian

$$E_{HF} = -\frac{11}{32}\sqrt{\frac{\pi}{2}} - \frac{1}{2}\beta\Delta_B + \frac{1}{\sqrt{2}\ell e}\beta\left(\Delta_B - \frac{1}{2}\Delta_B^{(1)}\right)p_z(0) \text{ « Zeeman » coupling}$$
$$+ \frac{1}{4e^2\ell^2} \sum_{\mathbf{q}} \mathbf{p}_{\parallel}(-\mathbf{q}) \cdot [a(q)\mathbf{I} + b(q)\Lambda(\mathbf{q})] \cdot \mathbf{p}_{\parallel}(\mathbf{q})$$
$$+ \frac{1}{4e^2\ell^2} \sum_{\mathbf{q}} c(q)p_z(-\mathbf{q})p_z(\mathbf{q}) \quad \begin{array}{l} \text{a and c: nonlocal exchange interactions} \\ \text{b: dipole-dipole electrostatic interaction} \end{array}$$
$$+ \frac{i}{8e^2\ell^2} \sum_{\mathbf{q}} d(q)(\hat{\mathbf{z}} \times \hat{\mathbf{q}}) \cdot (\mathbf{p}(-\mathbf{q}) \times \mathbf{p}(\mathbf{q})).$$

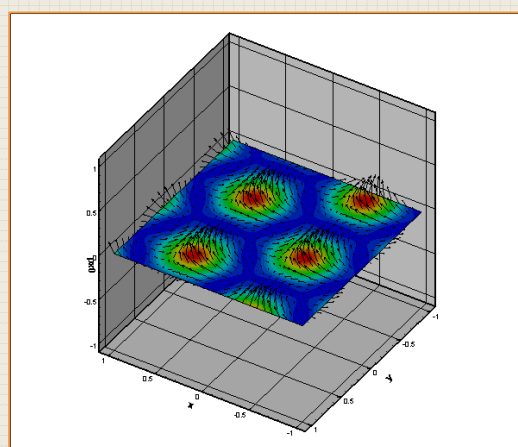
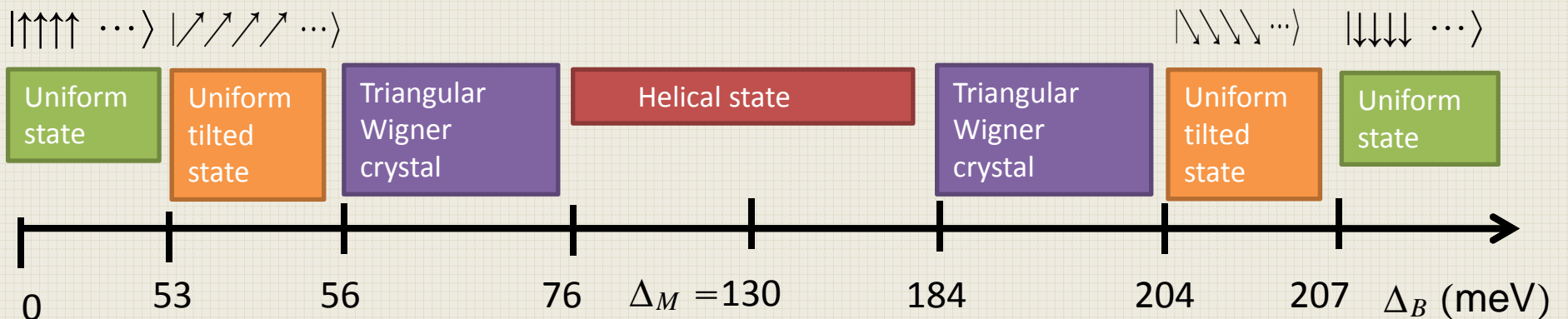
---

$$\sim D \int d\mathbf{r} (\mathbf{p} \cdot (\nabla \times \mathbf{p}))$$

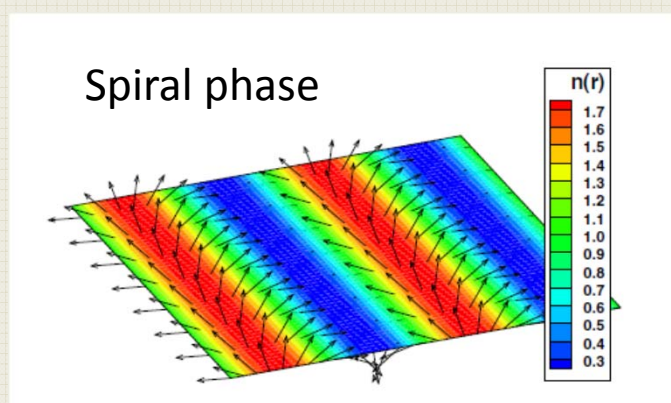
$\mathbf{p}$ = orbital pseudospin

Dzyaloshinski–Moriya interaction  
(from Coulomb interaction, not spin-orbit)

# Phase diagram for $\nu=3$



Wigner crystal  
with meron-like  
pseudospin texture

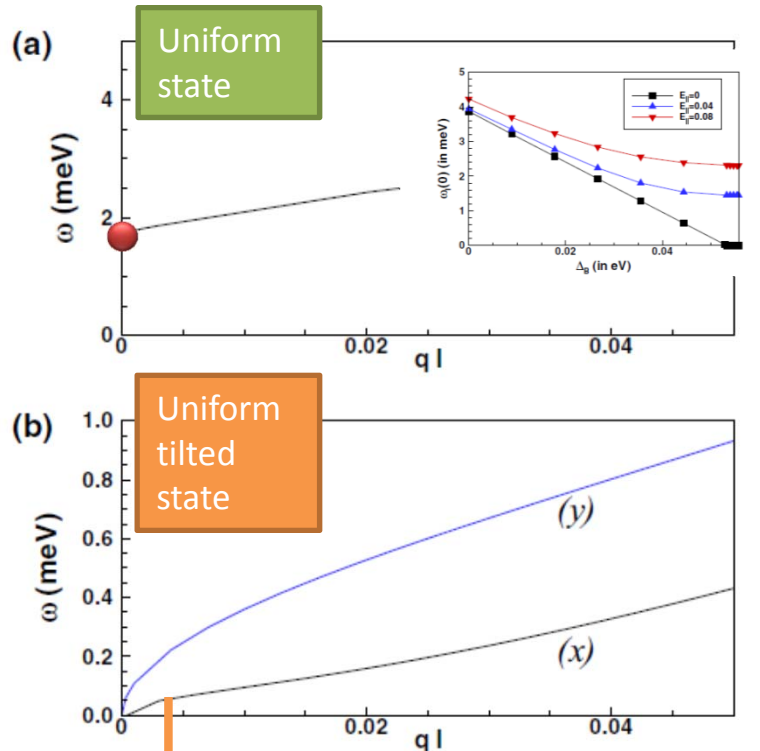


The electronic density  
is also modulated  
in space.

$$B = 10 \text{ T}$$

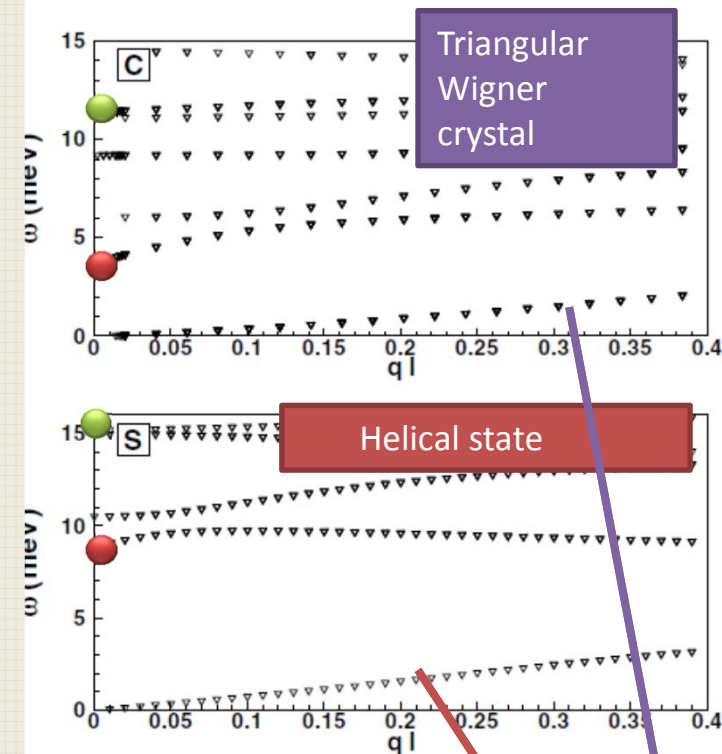
$$\varepsilon = 5$$

# Magnetoexciton modes



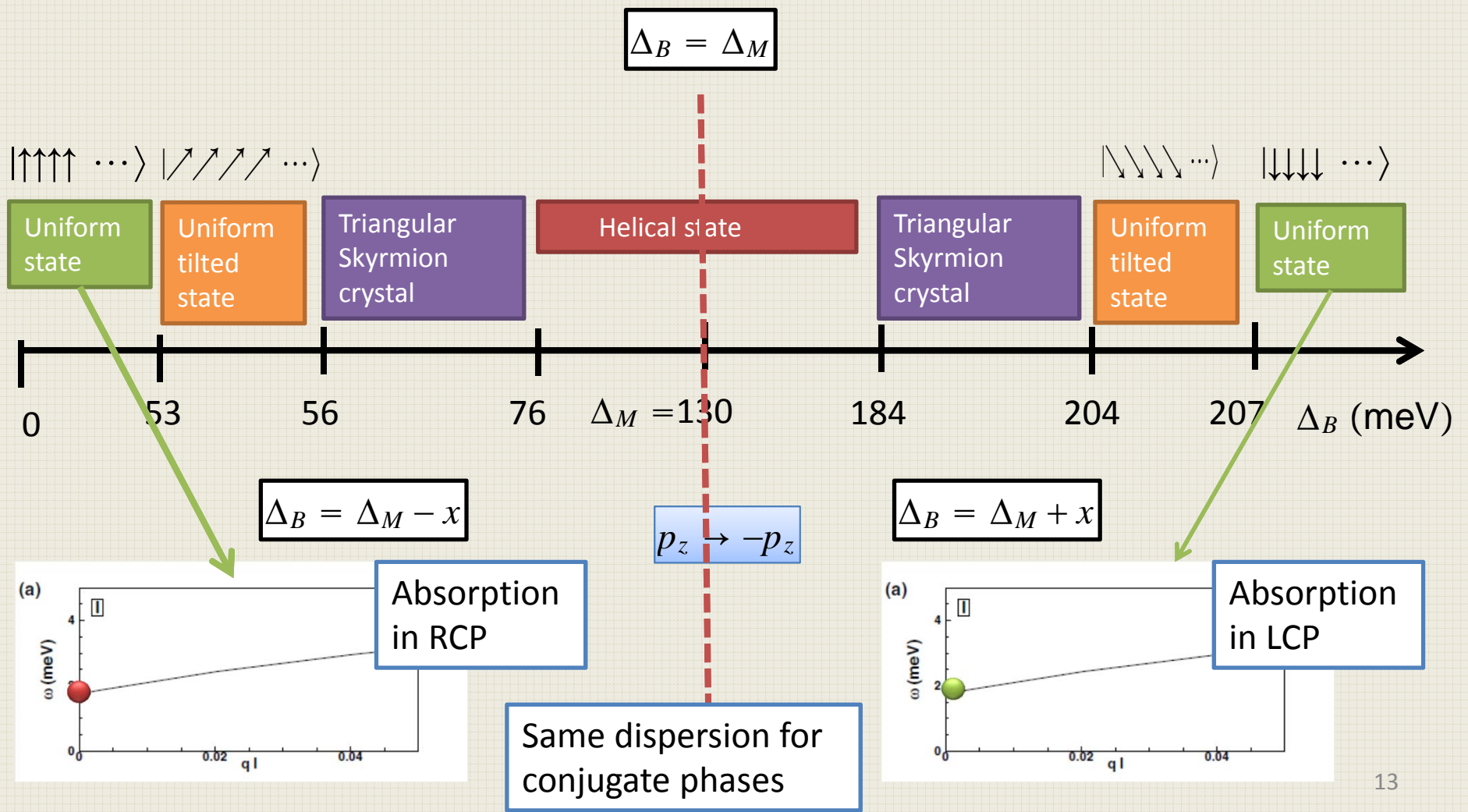
Goldstone mode with anisotropic dispersion

$$3.85 \text{ meV} \Rightarrow 9.3 \times 10^{11} \text{ Hz}$$

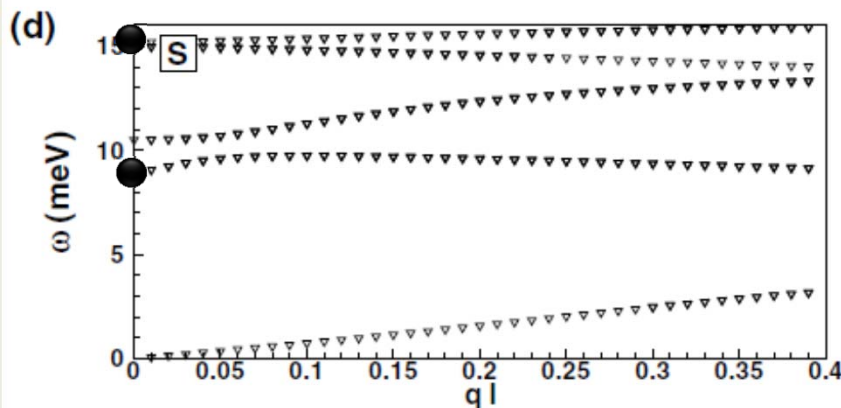


Gapless phonon mode in the WC and helical phases

# Symmetry of the phase diagram:conjugate states



# Optical absorption in helical state



$$\Delta_B = \Delta_M - x$$

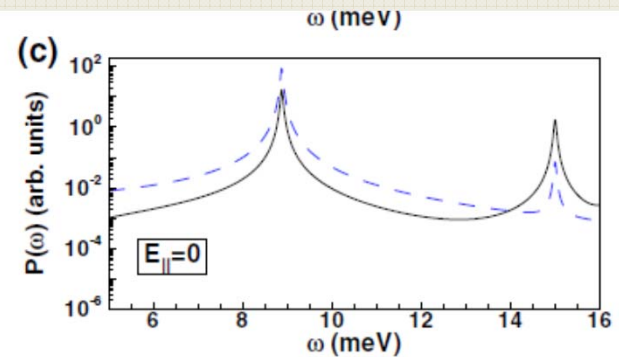
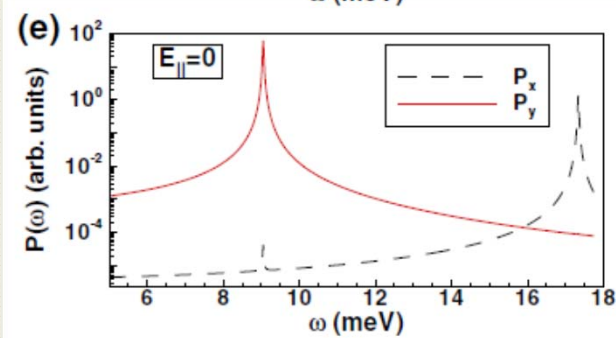
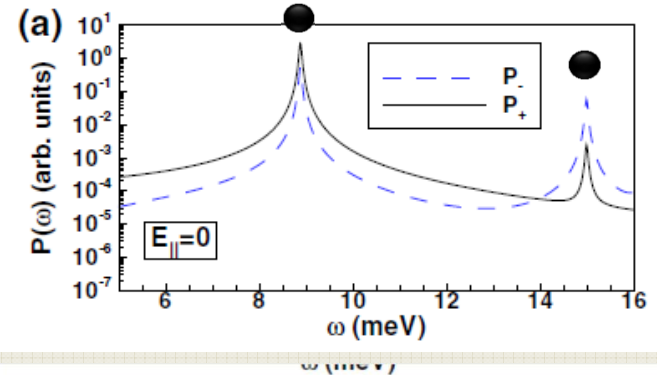
Modes are not fully circularly polarised.  
in helical state

linear polarisation for  $\Delta_B = \Delta_M$

Symmetry RCP-LCP for conjugate  
phases

$$\Delta_B = \Delta_M$$

$$\Delta_B = \Delta_M + x$$



# Kerr effect

Modes that are active in absorption also show a Kerr effect

Uniform state

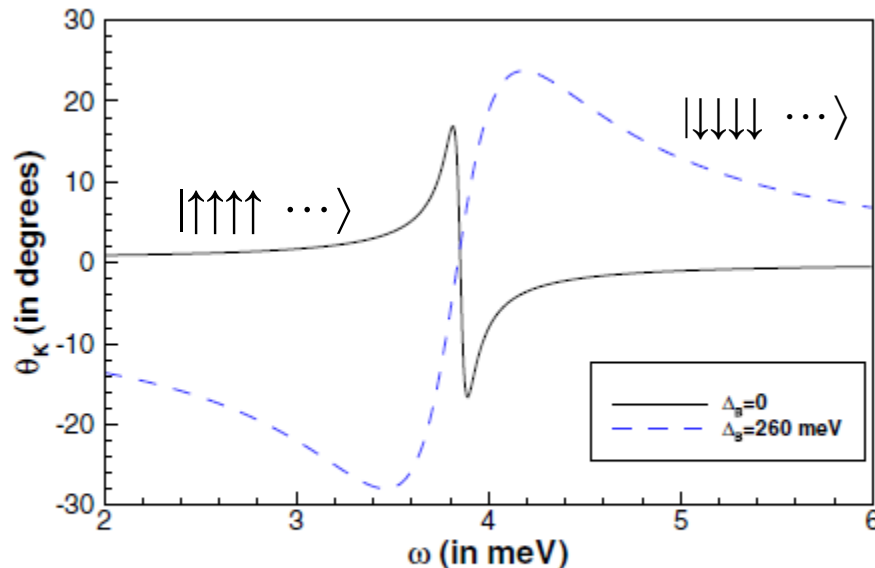


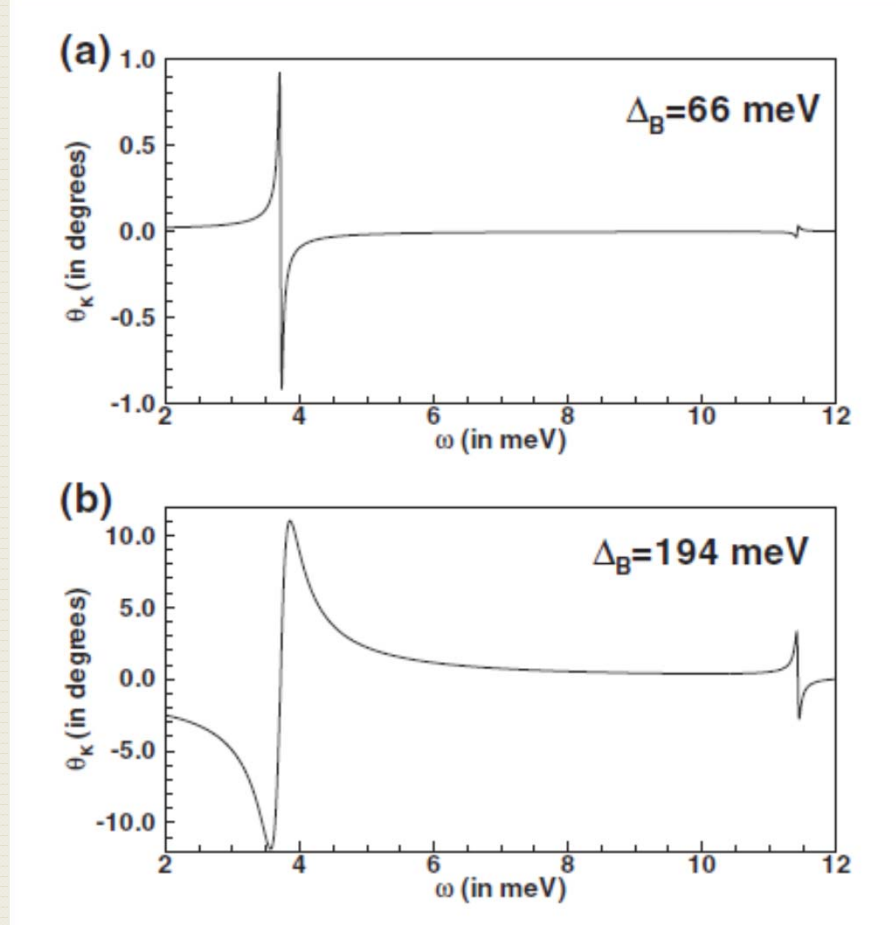
FIG. 12. (Color online) Kerr angle for conjugate biases  $\Delta_B = 0$  and  $\Delta_B = 260 \text{ meV}$  in the  $I$  and  $I^*$  phases.

Polarisation angle rotates in opposite directions for conjugate phases.

Also in the WC and helical phases.

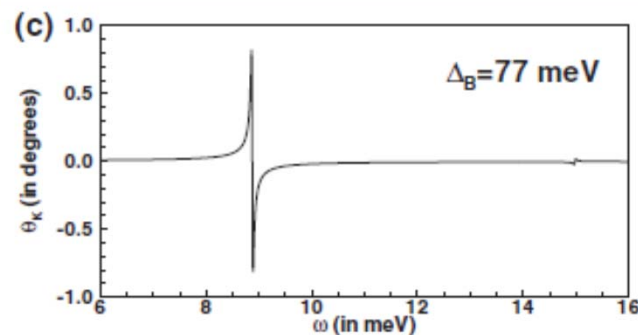
We have not included disorder so that we cannot obtain the numerical value of the Kerr angle.

# Kerr effect: skyrmion crystal

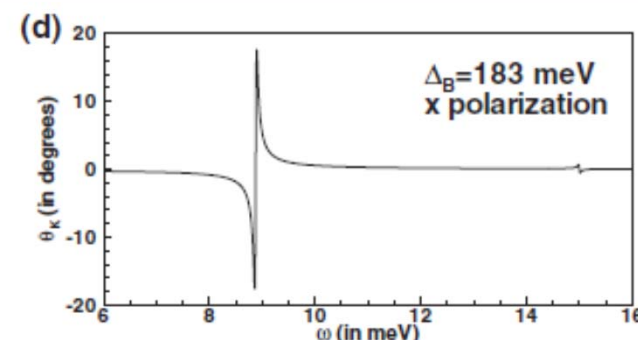


Polarisation angle rotates in the opposite direction in the conjugate phase.

# Kerr effect: helical state



Polarisation angle rotates in opposite directions for conjugate phases.



No Kerr effect at  $\Delta_B = \Delta_M$

# Conclusion

- ❖ At some special filling factors, the biased Bernal-stacked bilayer graphene behave as an helical ferromagnet.
- ❖ Several nonuniform phases are obtained as the bias is increased.
- ❖ All phases but one (the tilted state) have gapped magnetoexcitonic states, some of which are active in optical absorption and Kerr rotation. Conjugate phases are active in opposite circular polarisations and their Kerr angle rotate in opposite directions.

# Non-collinear spin configurations in helical ferromagnets

Magnetic field perpendicular to thin film plane

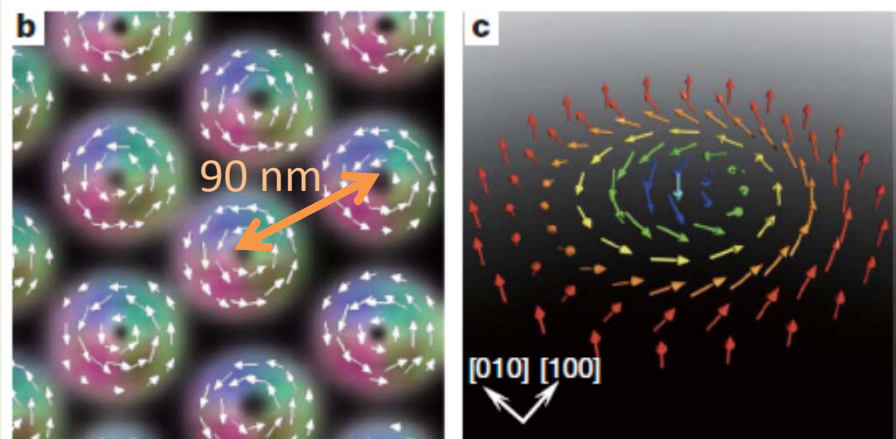
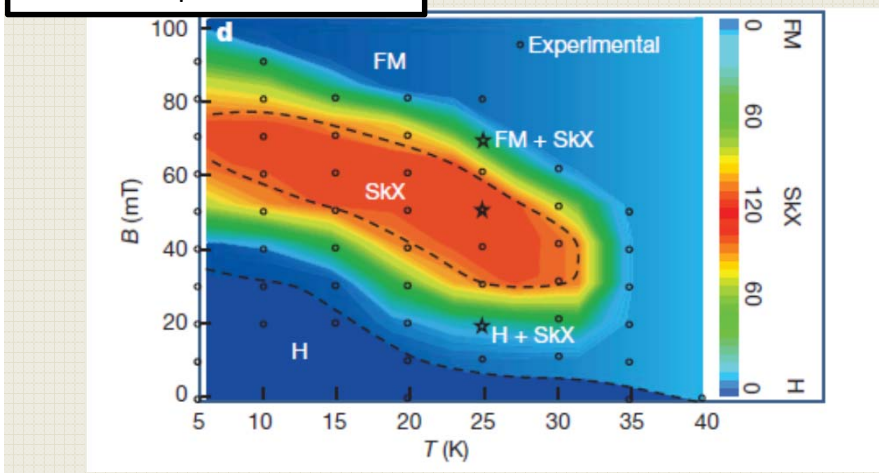


**Figure 3 | Phase diagrams of magnetic structure and spin textures in a thin film of  $\text{Fe}_{0.5}\text{Co}_{0.5}\text{Si}$ . a–c, Spin textures observed using Lorentz TEM**

Real-space imaging using  
Lorentz transmission electron microscopy

$$H = \int d\mathbf{r} \left[ \frac{J}{2} (\nabla M)^2 + \alpha M \cdot (\nabla \times M) \right]$$

Ferromagnetic exchange  
+ Dzyaloshinskii  
-Moriya interaction

**From X. Z. Yu et al., Nature Letters, 465, 901 (2010).**

We find a similar behavior with bias in Bernal-stacked bilayer graphene : an effective DM interaction arises from the Coulomb interaction and the magnetic moments are replaced by electric dipoles. The different phases are detectable in optical (absorption, Kerr) experiments.